

Dual-Band RF Rectifier Using Stepped Microstrip Line Matching Network for IOT Sensors Application

Meghdad Khodaei*, Halim Boutayeb, Larbi Talbi, and Alireza Ghayekhloo

School of Electrical Engineering, University of Quebec in Outaouais, Gatineau, Canada

ABSTRACT: RF rectifier circuits are critical to powering IOT sensors through energy harvesting process, allowing devices to operate without conventional batteries. This paper presents an efficient and dual-band RF rectifier circuit working at 0.915 GHz and 2.45 GHz frequencies which could be used in IOT power sensor devices. The design of a dual-band matching circuit, which is a key element of the RF rectifier, is discussed, and closed-form expressions are derived to extract the most significant parameters. In order to simplify the matching circuit, only three microstrip line sections are required in this design. The first line makes the structure independent of frequency, and the second and third lines are used to transfer the desired impedance to 50 Ohm of the source. For validation, a dual-band RF rectifier circuit using SMS7621-079LF Schottky diode is fabricated. The measured results show that the fabricated rectifier can achieve power conversion efficiency (PCE) around 65.7% and 62.4% (with a load resistance of 2500 Ohm and 5 dBm input power) at 0.915 GHz and 2.45 GHz, respectively. The dual-band and high-efficiency features of the proposed rectifier make it suitable for energy harvesting (EH) systems to power IOT sensor devices.

1. INTRODUCTION

Nowadays, internet of things (IOT) is becoming a more popular concept, due to its use to connect various devices and facilitate the everyday life. Sensors are an essential part of IOT. These sensors are used for a variety of applications, including smart cities, industrial automation, health care, and more. They are used to transmit and receive data and to monitor various systems. However, it is challenging to use these devices continuously, particularly in large-scale and remote areas, because of power deployment issue. Over the last few decades, the demand for energy harvesting technology has grown due to the rapid development of wireless devices and the growing use of wireless applications, such as wireless sensors and IOT. Sensors equipped by energy harvesting ensure reliable data collection by continuously monitoring environment conditions or infrastructure health without interruption [1–4]. Indeed, there is a clear potential to reduce pollution and feed sensors devices that do not have easy access to wired power through this method. RF energy harvester (RFEH) systems need antennas to capture the RF power from different sources, but in order to convert electromagnetic waves into usable DC voltage a rectifier circuit is required between the antenna and the load [5–10]. Using a wideband or multiband structure, more RF energy from the surrounding environment can be harvested than common single-band rectifiers. However, designing a wideband or multiband matching circuit can be challenging due to the changing input impedance of rectifier circuits with frequency, power level, and load resistance [11, 12]. However, more power conversion efficiency (PCE) can be attained by utilising the dual-band fea-

ture at desired frequencies as well [13–16]. In order to achieve dual-band rectifier circuit, a dual-band matching circuit has to be designed. A dual-band rectifier can be designed using two microstrip lines. However, this method is suitable for real load or impedance with low image part that is compensated by other circuit parts [17]. Dual-band performance is achieved by using multiple pairs of T-shaped stubs in [18]. However, it complicates the structure. Also, the combination of short and open circuit stub structures has been utilized to obtain dual-band performance in [19]. Dual-band matching circuit can also be designed using lumped elements [5, 20], but as frequencies increase, the efficiency of power conversion will degrade due to the lossy characteristics of capacitors and inductors. A dual-band rectifier circuit with operating frequencies of 1.4 GHz and 2.45 GHz has been constructed using a combination of lumped elements and modified T-section matching circuit in [21]. A dual-band microstrip rectifier with an extended dynamic range operating at 0.915 GHz and 2.45 GHz was reported in [22]. A dual-band rectifier circuit working at 2.4 GHz and 3.5 GHz was designed in [23], by combining L-type and Pi networks to make a dual-band matching, which increases the implementation complexity. However, these works require a complex design because of the number of microstrip and stub lines or the combination of lumped and distributed elements. In this work, a simple dual-band microwave matching circuit is utilized to develop a dual-band rectifier circuit. In order to achieve rectifying performance, only three cascaded microstrip lines are combined with a voltage doubler circuit. This results in a simple method of implementing a dual-band rectifier with high efficiency feature.

* Corresponding author: Meghdad Khodaei (khom13@uqo.ca).

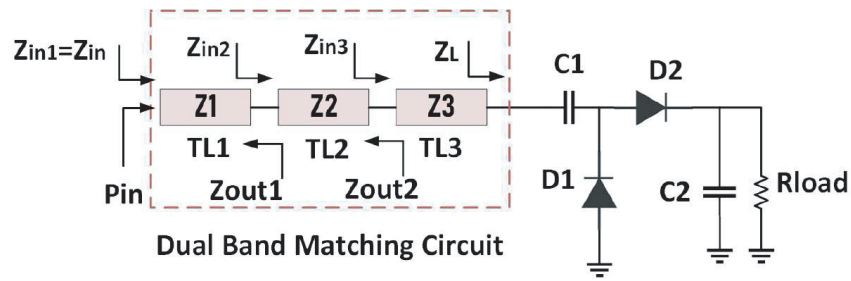


FIGURE 1. Schematic of proposed dual-band rectifier $W_{TL1} = 7.9$ mm, $W_{TL2} = 1$ mm, $W_{TL3} = 0.65$ mm $L_{TL1} = L_{TL2} = 15$ mm, $L_{TL3} = 30.8$ mm.

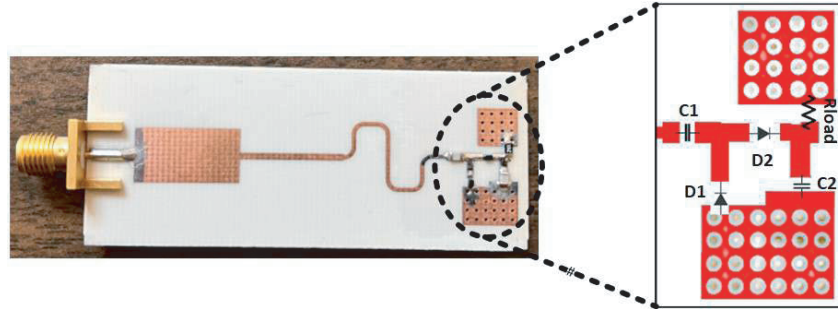


FIGURE 2. Fabricated proposed dual-band rectifier.

2. DESIGN AND ANALYSIS OF DUAL-BAND RECTIFIER

2.1. Schematic

Figure 1 shows the block diagram of the proposed dual-band rectifier circuit. It consists of a three-section microstrip line matching network (TL1-TL2-TL3), a DC block capacitor (C1), a DC pass filter (C2) to eliminate the harmonics and fundamental frequencies, two microwave Schottky diodes SMS7621-079LF (D1, D2), and a DC load (Rload). The voltage doubling configuration has been implemented with two diodes to achieve more output DC voltage. The frequencies selected for the design are 0.915 GHz and 2.45 GHz, which fall within the ISM (industrial, scientific and medical) band. The most critical parameter of the rectifier circuit is the input impedance of the doubler voltage, and its value depends on the RF input power, operating frequency, and terminating load (Rload). To determine the optimum load resistance and input power for both frequencies, a multi-frequency source pull simulation using Keysight Advanced Design System (ADS) software is performed initially. Then, the Harmonic Balance simulation should be used to determine Z_L at both frequencies. The final step in the process is to implement a dual-band matching circuit capable of converting Z_L to Z_{in} simultaneously at f_1 and f_2 . It is formed on a Rogers 4003 substrate ($\tan \delta = 0.0027$, substrate thickness: $H = 0.813$ mm). The layout of the fabricated circuit is shown in Figure 2.

2.2. Matching Network

Since Schottky diodes are nonlinear devices, their impedance varies with frequency and input power. Therefore, the input

impedance of a doubler voltage circuit is different at frequencies f_1 and f_2 . The dual-band three-section matching circuit, as shown in Figure 1, consists of a two-section transformer (Section 1 and Section 2 with lengths l_1 and l_2) and an additional Section 3 (with length l_3). In source pull simulation, $Z_{l1} = R_{l1} + jX_{l1}$ and $Z_{l2} = R_{l2} + jX_{l2}$ are considered as input impedances of this circuit at f_1 and f_2 , respectively ($f_1 > f_2$). TL3 is utilized to transform two unequal values and will eliminate the frequency-dependent character of the load impedance. For this, the input impedance at the input of TL3 at both frequencies should satisfy the following requirements:

$$\begin{aligned} Z_{in3}(f_1) &= Z_{in3}^*(f_2) \\ Z_{in3}(f_1, f_2) &= Z_{out2}^*(f_1, f_2) \\ Z_{in2}(f_1, f_2) &= Z_{out1}^*(f_1, f_2) \end{aligned} \quad (1)$$

In the first step, TL3 should be designed to match Z_{l1} and Z_{l2} to Z_{in3} :

$$Z_{in3}(f_1) = Z_3 \frac{R_{l1} + jX_{l1} + jZ_3 \tan(\beta_1 l_3)}{Z_3 + j(jX_{l1} + R_{l1}) \tan(\beta_1 l_3)} \quad (2)$$

$$Z_{in3}(f_2) = Z_3 \frac{R_{l2} + jX_{l2} + jZ_3 \tan(\beta_2 l_3)}{Z_3 + j(jX_{l2} + R_{l2}) \tan(\beta_2 l_3)} \quad (3)$$

Z_3 and l_3 are the impedance and length of TL3 that should be determined. β_1 and β_2 are the propagation constants at the two frequencies. Based on (1), (2) and (3) should be equal. By separating the real and imaginary parts, the following equations are obtained:

$$\begin{aligned} Z_3(1 - \tan(\beta_1 l_3) \tan(\beta_2 l_3))(R_{l1} - R_{l2}) \\ + (R_{l2} X_{l1} - R_{l1} X_{l2})(\tan(\beta_1 l_3) + \tan(\beta_2 l_3)) = 0 \end{aligned} \quad (4)$$

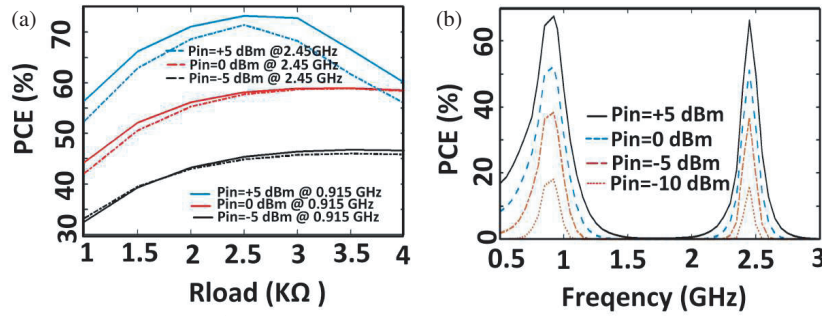


FIGURE 3. Parametric studies; (a) simulated PCE as a function of Rload at both 0.915 GHz and 2.45 GHz frequencies, and (b) measured PCE as a function of input power level.

$$(Z_3^2 - R_{l1}R_{l2} - X_{l1}X_{l2})(\tan(\beta_1 l_3) + \tan(\beta_2 l_3)) + Z_3(1 - \tan(\beta_1 l_3) \tan(\beta_2 l_3))(X_{l1} + X_{l2}) = 0 \quad (5)$$

Z_3 and l_3 can be calculated from these two equations. However, due to the imaginary parts present at the input impedance of the rectifier structure, let us assume that:

$$(1 - \tan(\beta_1 l_3) \tan(\beta_2 l_3)) \neq 0 \quad (6)$$

This condition avoids solutions with only real impedance at load. The equations can be solved easily based on this assumption (as mentioned, those parameters are important because they allow the structure to be independent of frequencies):

$$Z_3 = \sqrt{R_{l1}R_{l2} + X_{l1}X_{l2} + (X_{l2}R_{l1} - X_{l1}R_{l2}) \frac{X_{l1} + X_{l2}}{R_{l2} - R_{l1}}} \quad (7)$$

$$l_3 = \frac{n\pi + \arctan\left(\frac{z_3(R_{l1} - R_{l2})}{X_{l2}R_{l1} - X_{l1}R_{l2}}\right)}{(m + 1)\beta_1} \quad (8)$$

where $m = \frac{f_1}{f_2}$ and n could be chosen arbitrary, but fabricating issues should be considered.

In the second step of the design, the two cascaded microstrip lines convert $Z_{in} = 50 \Omega$ to Z_{in3} . The impedances at the inputs of TL2 and TL1 can be expressed:

$$Z_{in2} = Z_2 \frac{Z_{in3} + jZ_2 \tan(\beta_2 l_2)}{Z_2 + jZ_{in3} \tan(\beta_2 l_2)} \quad (9)$$

$$Z_{in1} = Z_{in} = Z_1 \frac{Z_{in2} + jZ_1 \tan(\beta_1 l_1)}{Z_1 + jZ_{in2} \tan(\beta_1 l_1)} \quad (10)$$

If $Z_{in3} = R_{in3} + jX_{in3}$, $Z_{in} = 50 \Omega$ and by combining (9) and (10), a new equation can be obtained. The real (and imaginary) parts of both sides of the equation can be equalized:

$$\begin{aligned} & -(R_{in3}Z_1^2 - Z_0Z_2^2) \tan(\beta_1 l_1) \tan(\beta_2 l_2) \\ & + X_{in3}Z_0(Z_1 \tan(\beta_2 l_2) + Z_2 \tan(\beta_1 l_1)) \\ & + Z_1Z_2R_{in3} - Z_1Z_2Z_0 = 0 \end{aligned} \quad (11)$$

$$\begin{aligned} & -Z_1^2Z_2 \tan(\beta_1 l_1) - Z_2^2Z_1 \tan(\beta_2 l_2) \\ & - Z_1Z_2Z_{in3} + R_{in3}Z_0(Z_1 \tan(\beta_2 l_2) + Z_2 \tan(\beta_1 l_1)) \\ & + X_{in3} \tan(\beta_1 l_1) \tan(\beta_2 l_2) = 0 \end{aligned} \quad (12)$$

It should be considered that each equation is for two frequencies. In this way, the length and characteristic impedance of TL1 and TL2 are determined to convert the independent impedance at the input of TL3 to source impedance of 50Ω . In order to calculate the characteristic impedances of TL1 and TL2, a fourth term equation needs to be solved by numerical or optimization methods, but the length of these lines is calculated as follows:

$$l_1 = l_2 = \frac{\pi}{\beta_1 + \beta_2} \quad (13)$$

Finally, using MATLAB software Z_1 , Z_2 are obtained easily by derived equation [24]. This analytical approach combined with tuning using ADS software achieves the dual-band matching circuit illustrated in Figure 2.

3. RESULTS AND DISCUSSION

A dual-band matching circuit has been designed to deliver the maximum power from antenna to the output load at two different frequencies. Microstrip lines with optimal physical dimensions are shown in Figure 1. However, meandering has been done on TL3 to compact the whole structure. PCE as the most important parameter of rectifier circuits is defined as follows:

$$\gamma = \frac{P_{DC}}{P_{in}} = \frac{V_{out}^2}{R_{load}P_{in}} \times 100\% \quad (14)$$

where V_{out} is the DC output voltage, P_{in} the input power level, and R_{load} the load resistance. The PCE versus load resistance plotted in Figure 3(a) shows that $2.5 \text{ k}\Omega$ is the optimal load resistance for the best performance of the rectifier. Also, Figure 3(b) illustrates the PCE as a function of frequency at different input power levels. The results demonstrate that 54.7% and 51.3% PCE can be generated at 0.915 GHz and 2.45 GHz, respectively at the input power of 0 dBm. By increasing the input power to 5 dBm, PCE will go up to 65.7% and 62.4% at 0.915 GHz and 2.45 GHz, respectively. The rectifier's impedance matching performance is depicted in Figure 4. As can be observed, over a broad input power range, excellent matching was attained. These parameters can be measured by applying power to the input of the circuit by RF signal source and measuring the output voltage across the load by multimeter. This test setup and simulated and measured results for PCE and

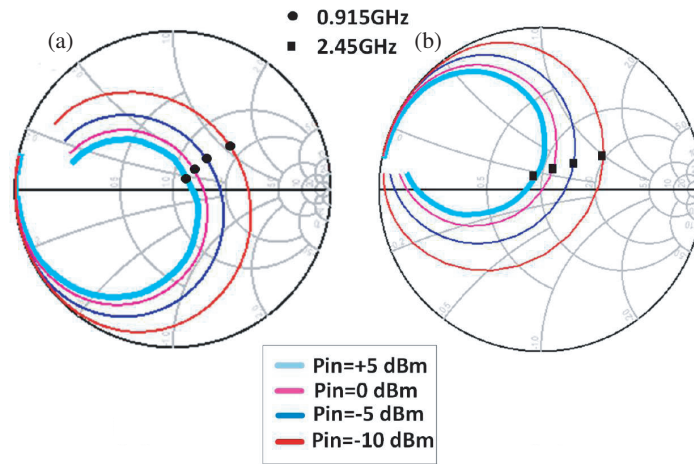


FIGURE 4. Input impedance of proposed rectifier at different input power level (a) from 0.8 GHz to 1.8 GHz (b) 1.8 GHz to 2.6 GHz.

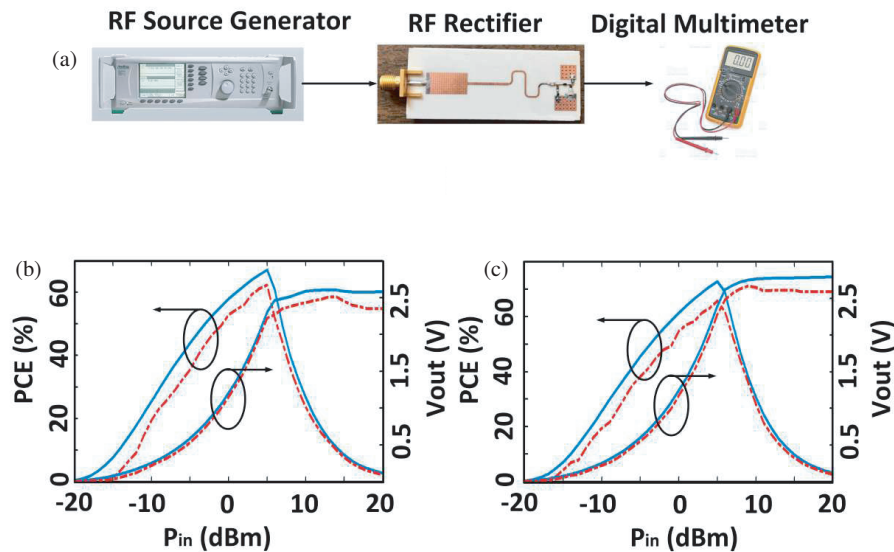


FIGURE 5. Experimental procedure; (a) measurement test setup, and (b) simulated and measured results of PCE alongside V_{out} versus input power at 0.915 GHz and $R_{load} = 2.5 \text{ k}\Omega$, (c) simulated and measured results of PCE alongside V_{out} versus input power at 2.45 GHz and $R_{load} = 2.5 \text{ k}\Omega$.

output voltage as a function of the input power level at both frequencies are illustrated in Figure 5. It has been measured that PCE can reach 65.7% and 62.4% at 0.915 GHz and 2.45 GHz with 5 dBm input power, respectively. Following this point, the efficiency of the diode begins to decline dramatically as a result of its behaviour when being subjected to high power levels. The measured output voltage at both frequencies is over 1.2 V after reaching 0 dBm input power, and at maximum efficiency, it is around 2.3 V and 2.2 V at 0.915 GHz and 2.45 GHz, respectively. Figure 6 shows the simulated and measured reflection coefficients and PCEs at 5 dBm input power for both frequencies. It is shown that this amount is better than -14 dB , and it confirms that reasonable matching performance has been realized at both frequencies. It is better to take into consideration that diode nonlinearity specification and intermodulation products are two inevitable phenomena that may decrease efficiency and are not eliminated by a DC output filter. Moreover, a small difference is observed between simulated and measured results,

due to the Schottky diode model inaccuracy and fabrication tolerance. Table 1 compares the performances of the proposed design and those of existing dual-band rectifiers from the literatures. In comparison with other works, using a simple three-section stepped microstrip line impedance transformer, a dual-band rectifier with reasonable performance is achieved. Compared to other studies, the number of transmission lines used in this study is less, which is an important factor in reducing microstrip line parameters sensitivity. The parameters tolerances are easily compensated, and open and short stubs are not used, since they introduce a greater level of sensitivity [18, 23]. It is common to use the lumped elements to design the dual-band rectifiers in some literatures [5, 21], but quality factor has a significant influence on the circuit performance, and it may vary depending on the topology. However, the suggested circuit eliminates the need for these types of components. As a result, a simpler method to implement a dual-band rectifier with high efficiency feature has been proposed.

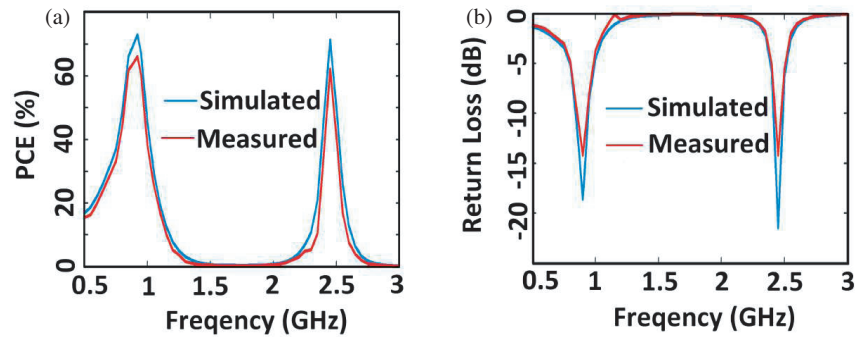


FIGURE 6. Measured and simulated results of proposed rectifier at $P_{in} = 5$ dBm and $R_{load} = 2.5$ k Ω . (a) PCE. (b) Return loss.

TABLE 1. Comparison between the proposed rectifier and references.

Ref.	Diode Type	Frequency (GHz)	Peak Efficiency (%)	Input Power (cdBm)	No. of TL
[5]	CMOS	0.93/2.63	25.2/22.5	-1	LC
[13]	HSMS-2862	0.915/2.45	77.2/73.5	14.6	5
[14]	HSMS-2860	3.5/5.8	65/48.8	9.5/5	4
[18]	HSMS-285C	1.8/2.45	70/68	9	7
[21]	SMS7630	1.4/2.45	65/57	0	LC
[23]	SMS7621-079LF	2.32/3.48	64.5/64.2	5	8
This Work	SMS7621-079LF	0.915/2.45	65.7/62.4	5	3

4. CONCLUSION

In this paper, a novel dual-band impedance transformer using stepped microstrip line technique for the design of a high efficiency and dual-band rectifier with a doubler voltage configuration is presented. The initial parameters have been analyzed and estimated using closed-form expressions. Based on the parametric studies and analytical solution, a prototype has been fabricated, and experimental results have been reported to validate the proposed concept. According to the results, the proposed structure covers both frequencies of 0.915 GHz and 2.45 GHz with PCEs (at 5 dBm input power) of 65.7% and 62.4%, respectively. However, PCE is still more than 50% with 0 dBm input power. Also, the obtained impedance matching results are reasonable and less than -14 dBm at both frequencies. As a result of the circuit performance, it can be a good candidate to integrate with an antenna to receive power and used as an energy harvester.

REFERENCES

- [1] Kashyap, N., Geetanjali, and D. Singh, "A novel circularly polarized annular slotted multiband rectenna for low power sensor applications," *Progress In Electromagnetics Research B*, Vol. 99, 103–119, 2023.
- [2] Mehta, P. and A. Nella, "A quad-band low power high sensitive RF to DC converter circuit for RF energy harvesting applications," *Progress In Electromagnetics Research M*, Vol. 119, 189–201, 2023.
- [3] Bajtaoui, M., O. E. Mrabet, M. A. Ennasar, and M. Khalladi, "A novel circular polarized rectenna with wide ranges of loads for wireless harvesting energy," *Progress In Electromagnetics Research M*, Vol. 106, 35–46, 2021.
- [4] Surender, D., M. A. Halimi, T. Khan, F. A. Talukdar, S. K. Koul, and Y. M. M. Antar, "2.45 GHz Wi-Fi band operated circularly polarized rectenna for RF energy harvesting in smart city applications," *Journal of Electromagnetic Waves and Applications*, Vol. 36, No. 3, 407–423, 2022.
- [5] Li, C.-H., M.-C. Yu, and H.-J. Lin, "A compact 0.9-/2.6-GHz dual-band RF energy harvester using SiP technique," *IEEE Microwave and Wireless Components Letters*, Vol. 27, No. 7, 666–668, 2017.
- [6] Quddious, A., S. Zahid, F. A. Tahir, M. A. Antoniadis, P. Vryonides, and S. Nikolaou, "Dual-band compact rectenna for UHF and ISM wireless power transfer systems," *IEEE Transactions on Antennas and Propagation*, Vol. 69, No. 4, 2392–2397, 2020.
- [7] Yoshida, S., N. Hasegawa, and S. Kawasaki, "The aerospace wireless sensor network system compatible with microwave power transmission by time-and frequency-division operations," *Wireless Power Transfer*, Vol. 2, No. 1, 3–14, 2015.
- [8] Collado, A. and A. Georgiadis, "Conformal hybrid solar and electromagnetic (EM) energy harvesting rectenna," *IEEE Transactions on Circuits and Systems I: Regular Papers*, Vol. 60, No. 8, 2225–2234, 2013.
- [9] He, Q. and C. Liu, "An enhanced microwave rectifying circuit using HSMS-282," *Microwave and Optical Technology Letters*, Vol. 51, No. 4, 1151–1153, 2009.
- [10] Song, C., Y. Huang, J. Zhou, J. Zhang, S. Yuan, and P. Carter, "A high-efficiency broadband rectenna for ambient wireless energy harvesting," *IEEE Transactions on Antennas and Propagation*, Vol. 63, No. 8, 3486–3495, 2015.
- [11] Guo, L., X. Li, W. Sun, W. Yang, Y. Zhao, and K. Wu, "Designing and modeling of a dual-band rectenna with compact dielectric resonator antenna," *IEEE Antennas and Wireless Propagation*

- tion Letters, Vol. 21, No. 5, 1046–1050, 2022.
- [12] Lin, Y. L., X. Y. Zhang, Z.-X. Du, and Q. W. Lin, “High-efficiency microwave rectifier with extended operating bandwidth,” *IEEE Transactions on Circuits and Systems II: Express Briefs*, Vol. 65, No. 7, 819–823, 2017.
- [13] Liu, J., X. Y. Zhang, and C.-L. Yang, “Analysis and design of dual-band rectifier using novel matching network,” *IEEE Transactions on Circuits and Systems II: Express Briefs*, Vol. 65, No. 4, 431–435, 2017.
- [14] Halimi, M. A., T. Khan, S. K. Koul, and S. R. Rengarajan, “A dual-band rectifier using half-wave transmission line matching for 5G and Wi-Fi bands RFEH/MPT applications,” *IEEE Microwave and Wireless Technology Letters*, Vol. 33, No. 1, 74–77, 2022.
- [15] Wang, M., Y. Fan, L. Yang, Y. Li, J. Feng, and Y. Shi, “Compact dual-band rectenna for RF energy harvest based on a tree-like antenna,” *IET Microwaves, Antennas & Propagation*, Vol. 13, No. 9, 1350–1357, 2019.
- [16] Nguyen, D.-A. and C. Seo, “A compact and high-efficiency design of 0.915/2.45 GHz dual-band shunt-diode rectifier for wireless power transfer,” *IEEE Microwave and Wireless Components Letters*, Vol. 32, No. 7, 915–918, 2022.
- [17] Khodaei, M., H. Boutayeb, and L. Talbi, “High efficiency and dual-band RF rectifier circuit for energy harvesting systems,” in *2023 IEEE International Symposium on Antennas and Propagation and USNC-URSI Radio Science Meeting (USNC-URSI)*, 671–672, Portland, OR, USA, Jul. 2023.
- [18] Chandravanshi, S. and M. J. Akhtar, “An efficient dual-band rectenna using symmetrical rectifying circuit and slotted monopole antenna array,” *International Journal of RF and Microwave Computer-Aided Engineering*, Vol. 30, No. 4, e22117, 2020.
- [19] Sun, H., Y.-x. Guo, M. He, and Z. Zhong, “A dual-band rectenna using broadband Yagi antenna array for ambient RF power harvesting,” *IEEE Antennas and Wireless Propagation Letters*, Vol. 12, 918–921, 2013.
- [20] Niotaki, K., A. Georgiadis, A. Collado, and J. S. Vardakas, “Dual-band resistance compression networks for improved rectifier performance,” *IEEE Transactions on Microwave Theory and Techniques*, Vol. 62, No. 12, 3512–3521, 2014.
- [21] Dubey, R., S. K. Srivastava, A. Singh, and M. K. Meshram, “Compact and efficient dual-band rectifier using modified T-section matching network,” *IEEE Microwave and Wireless Technology Letters*, Vol. 33, No. 6, 755–758, 2023.
- [22] Huang, M., Y. L. Lin, J.-H. Ou, X. y. Zhang, Q. W. Lin, W. Che, and Q. Xue, “Single-and dual-band RF rectifiers with extended input power range using automatic impedance transforming,” *IEEE Transactions on Microwave Theory and Techniques*, Vol. 67, No. 5, 1974–1984, 2019.
- [23] Bui, G. T., D.-A. Nguyen, and C. Seo, “A novel design of dual-band inverse class-F shunt-diode rectifier for energy harvesting,” *IEEE Transactions on Circuits and Systems II: Express Briefs*, Vol. 70, No. 7, 2345–2349, 2023.
- [24] Liu, X., Y. Liu, S. Li, F. Wu, and Y. Wu, “A three-section dual-band transformer for frequency-dependent complex load impedance,” *IEEE Microwave and Wireless Components Letters*, Vol. 19, No. 10, 611–613, 2009.